Advanced Meta-Modelling Techniques and Sensitivity Analysis for Rotordynamics in an Uncertain Context

Enora Denimal, Jean-Jacques Sinou

Advanced Meta-Modelling Techniques and Sensitivity Analysis for Rotordynamics in an Uncertain Context

E. Denimal[a], J-J. Sinou[b,c]
a. Univ. Gustave Eiffel, Inria, COSYS/SII, I4S, Campus Beaulieu, Rennes, France – enora.denimal@inria.fr
b. Lab. Tribologie et Dynamique des Systèmes, UMR CNRS 5513, Ecole Centrale de Lyon, Ecully, France
c. Institut Universitaire de France, Paris, France

ABSTRACT
It is essential to predict accurately the critical speeds and associated vibration amplitudes of rotating machineries to ensure a correct design to limit noise nuisance and fatigue failure. However, numerous uncertainties are present, due to environmental variations or manufacturing tolerances for e.g., and must be taken into consideration in the design stage to limit their impact on the system dynamics. These uncertainties are usually modelled with a probability law and the dynamic response becomes stochastic. On the other side, during the design stage, a few key parameters, often called design parameters, are identified and tuned to ensure a robust conception of the rotor w.r.t to the uncertain model parameters. In this context, one must tackle a high-dimension parametric problem but numerous parameters of different nature. The efficiency of an advanced meta-modelling technique that couple polynomial chaos expansion and kriging is demonstrated here. The kriging efficiency is improved by introducing physical properties of the rotor. A finite element model of a rotor subjected to nine uncertain parameters is studied. The hybrid surrogate model gives a direct access to the Sobol indices, exploited to conduct an extensive sensitivity analysis.

Keywords : rotordynamics, hybrid uncertainties, kriging, polynomial chaos expansion, Sobol indices

INTRODUCTION

Rotors are main components in many applications, such as for transports or energy production. They must be able to carry out important loadings, and so their design must be undertaken carefully. More particularly, dramatic accidents and failures may occur due to the vibrational loadings and so the vibration analysis of such components is primordial to reduce noise and failures due to vibrational loadings. In this context, the prediction of the critical speeds and associated vibration amplitudes are the main concern of engineers during the design to ensure that the vibrations that the rotor will endure are acceptable. Being able to predict accurately and robustly these critical speeds and vibration amplitudes to detect potential issues are of major concern in the design stage. This task is complex as rotors depend on many parameters (geometry, material, bearings etc) making difficult to get a global vision of the dynamic of the structure and the impact of the variability that each component would have on the global response. Thus, one of the most difficult problem nowadays is to develop methods that integrate these uncertainties and are numerically applicable to large and realistic mechanical systems.

When designing such systems, engineers are facing many uncertainties that can be of different natures. They can usually be split into two groups. The first group corresponds to design parameters, i.e. parameters that are usually tuned by engineers and used for the conception of the rotor. They often take value in an interval and parametric studies are conducted to tune them. The second group corresponds to uncertain parameters, i.e. parameters that translate a variability or a lack of knowledge due to tolerances, environmental fluctuations etc. They are often modelled by probability density functions. When many uncertain parameters are present, an efficient strategy consists in the creation of a surrogate model that mimics the behaviour of the full model. Recent strategies have been based on the use of a single method, as PCE [1,2,3] or kriging [4,5,6] to predict the critical speeds of uncertain rotors. However, none of them is able to deal with both nature of uncertainty at this step. In this context, a recent approach has been developed that combines PCE and kriging to model both random and parametric uncertainties [7]. This method has

given good results applied for the prediction of friction-induced vibrations for both academic models and industrial models [7,8].

This work proposes to predict the dynamic behaviour of a rotor subjected to numerous uncertainties of different natures. More precisely, two of them are parametric and seven others are random. The efficiency of the hybrid surrogate model is demonstrated on this case. The prediction of the mean and variances of the critical speeds and amplitudes is performed, and the formulation avoid costly MCS simulations thus reducing the numerical cost. Moreover, a sensitivity analysis of the rotor is conducted and complex behaviours are analysed. Finally, the kriging part is improved by introducing the symmetrical properties of the rotor in the formulation.

The paper is organised as follows. First, the model under study is briefly presented. Then the hybrid surrogate model is presented. Specifications on an efficient construction of the kriging are also given. Finally, the efficiency and accuracy of the hybrid surrogate model to predict the critical speeds and associated vibration amplitudes are demonstrated. Additionally, a sensitivity analysis based on the Sobol indices is conducted to get deep insights in the rotor dynamics.

DESCRIPTION OF THE ROTOR

This section describes briefly the rotor modelling. It is composed of a shaft supported by two bearings and four discs as represented in Figure 1. An unbalanced mass is located on the first disc. For a detailed description of the construction of the model, the interested reader can refer to [5,9,10].

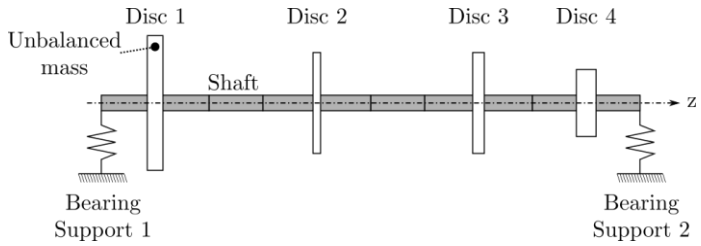

Figure 1: Rotor under study

The shaft is modelled with a Finite Element Model (FEM) of ten Euler beams. Each node has four degrees of freedom (2 displacements and 2 rotations) and nodal displacements of the element *i*th are denoted $\mathbf{x}^{(s,i)}$. The EOM of the *i*th element writes:

$$\left(\mathbf{M}_R^{(s,l)} + \mathbf{M}_T^{(s,l)}\right)\ddot{\mathbf{x}}^{(s,i)} + \left(\mathbf{C}^{(s,l)} + \omega\mathbf{G}^{(s,l)}\right)\dot{\mathbf{x}}^{(s,i)} + \mathbf{K}^{(s,l)}\mathbf{x}^{(s,i)} = \mathbf{0}$$

with $\mathbf{M}_R^{(s,l)}$ and $\mathbf{M}_T^{(s,l)}$ the rotational and translational mass matrices of the element *i*th, $\mathbf{C}^{(s,l)}$ the damping matrix the element *i*th, $\mathbf{G}^{(s,l)}$ the gyroscopic matrix the element *i*th and $\mathbf{K}^{(s,l)}$ the stiffness matrix the element *i*th. Material properties of the shaft are summarized in Table 1.

The discs are modelled as rigid discs and the nodal displacement in the fixed frame is denoted $\mathbf{x}^{(d,j)}$. The EOM writes:

$$\left(\mathbf{M}_R^{(d,j)} + \mathbf{M}_T^{(d,j)}\right)\ddot{\mathbf{x}}^{(d,j)} + \omega\mathbf{G}^{(d,j)}\dot{\mathbf{x}}^{(d,j)} = \mathbf{F}^{(d,j)}$$

with $\mathbf{M}_R^{(d,j)}$ and $\mathbf{M}_T^{(d,j)}$ the rotational and translational mass matrices of the *j*th disc, $\mathbf{G}^{(d,j)}$ the gyroscopic matrix of the *j*th disc and $\mathbf{F}^{(d,j)}$ the unbalance of the disc *j*, of the form:

$$\mathbf{F}^{(d,j)} = [m_u d_u \omega^2 \cos\omega t + \phi \quad m_u d_u \omega^2 \sin\omega t + \phi \quad 0 \quad 0\ ]^T$$

with m_u the unbalanced mass, d_u the eccentricity of the mass, ϕ the initial phase and ω the rotational speed of the rotor. The different properties are summarized in Table 1.

Each flexible bearing supports is modelled as two linear springs, one in each direction of the fixed frame. They are denoted $k_v^{(b,1)}$, $k_h^{(b,1)}$, $k_v^{(b,2)}$ and $k_h^{(b,2)}$. The global matrices are $\mathbf{K}^{(b,1)}$ and $\mathbf{K}^{(b,2)}$.

The general dynamic equation of the rotor is:

$$\mathbf{M}\ddot{\mathbf{x}} + (\mathbf{C} + \omega\mathbf{G})\dot{\mathbf{x}} + \mathbf{K}\mathbf{x} = \mathbf{F}$$

where $\mathbf{M}$ groups the mass matrix of the shaft and the discs, $\mathbf{C}$ groups the damping matrix of the shaft, $\mathbf{G}$ groups the gyroscopic of the shaft and the discs, $\mathbf{K}$ groups the stiffness matrix of the shaft and the bearings and $\mathbf{F}$ is the vector of the unbalanced forces. For a detailed description of the matrix construction, the interested reader could refer to [5,10].

Finally, the Campbell diagram of the rotor is given in Figure 2 for different values of bearing stiffness of the second bearing. One can observe the impact of the bearing stiffnesses on the critical speeds.

Notation	Parameter name	Value
R_1	Outer radius – Disc 1	0.25 m
e_1	Thickness – Disc 1	0.03 m
R_2	Outer radius – Disc 2	0.1875 m
e_2	Thickness – Disc 2	0.015 m
R_3	Outer radius – Disc 3	0.1875 m
e_3	Thickness – Disc 3	0.0225 m
R_4	Outer radius – Disc 4	0.125 m
e_4	Thickness – Disc 4	0.0375 m
E_d	Young modulus of disc material	2.1 10^{11} N/m^2
ρ_d	Density of disc material	7800 kg/m^3
m_u	Mass unbalance – Disc 1	0.01 kg
d_u	Eccentricity of the unbalance mass – Disc 1	0.01 m
$k_h^{b,1}$	Horizontal stiffness – Bearing 1	3 10^6 N/m
$k_v^{b,1}$	Vertical stiffness – Bearing 1	3 10^6 N/m
$k_h^{b,2}$	Horizontal stiffness – Bearing 2	[0.1;2] 10^6 N/m
$k_v^{b,2}$	Vertical stiffness – Bearing 2	[0.1;2] 10^6 N/m

Table 1: Geometrical and material properties of the rotor

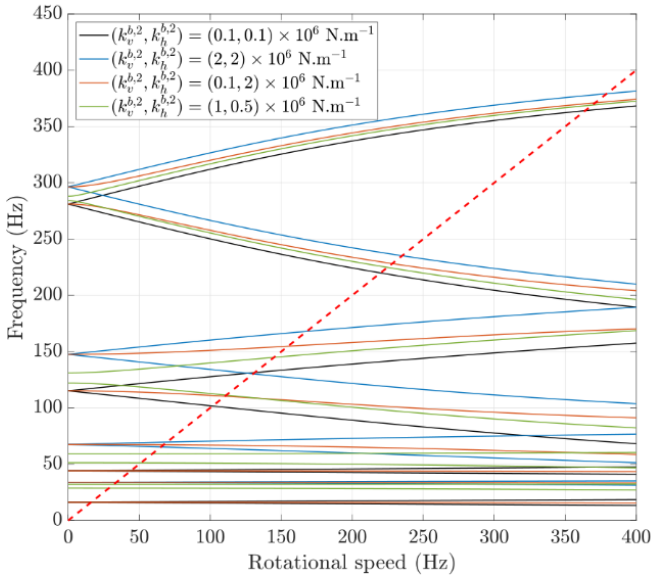

Figure 2: Campbell diagram for different second bearing stiffness

HYBRID SURROGATE MODEL

In this section, the uncertain parameters are presented first. Then, the methodology for uncertainty propagation is presented.

Uncertain parameters

Two types of uncertain parameters are considered here. The first set of uncertain parameters are random parameters and are described by a Probability Density Function (PDF). They might come from manufacturing tolerances or environmental variations for example. Seven parameters are in this group and are summarized in Table 2. Their influence on the model matrices depends on the parameter. They are grouped in the random vector $\boldsymbol{\xi} = \left[\xi_E, \xi_{e_1}, \xi_{e_2} \xi_{e_3}, \xi_{e_4}, \xi_{k_v^{(b,1)}}, \xi_{k_h^{(b,1)}}\right]$.

The second type of uncertain parameters are considered as deterministic and corresponds to the stiffness of the second bearing ($k_v^{(b,2)}$ and $k_h^{(b,2)}$) and can take value in [0.1;2] 10^6 N/m. They are grouped in the vector $\mathbf{x} = \left[k_v^{(b,2)}, k_h^{(b,2)}\right]$.

The final objective is to predict the rotor forward and backward critical speeds and associated vibration amplitudes when these two bearings stiffness vary and by taking into consideration the uncertainty of the seven random parameters. The critical speeds are denoted f^i and the associated vibration amplitudes a^i, for *i* in [1,8]. As they depend on $\mathbf{x}$ and $\boldsymbol{\xi}$, they can also be written: $f^i(\mathbf{x}, \boldsymbol{\xi})$ and $a^i(\mathbf{x}, \boldsymbol{\xi})$.

Notation	Parameter name	% variation	Law
E	Young modulus shaft	$\pm 5\%$	Uniform
e_1	Thickness – Disc 1	$\pm$ 10%	Uniform
e_2	Thickness – Disc 2	$\pm$ 10%	Uniform
e_3	Thickness – Disc 3	$\pm$ 10%	Uniform
e_4	Thickness – Disc 4	$\pm$ 10%	Uniform
$k_h^{b,1}$	Horizontal stiffness – Bearing 1	$\pm 5\%$	Uniform
$k_v^{b,1}$	Vertical stiffness – Bearing 2	$\pm 5\%$	Uniform

Table 2: Properties of the random parameters

Polynomial chaos

The random part of each quantity of interest (QoI) can be approximated by a convergent PCE of the form [11,12]:

$$\mathrm{Y}(\boldsymbol{\xi}) = \sum_{k=0}^{P-1} \alpha_k \Phi_k(\boldsymbol{\xi})$$

Where Y is the considered QoI (one critical speed or one vibration amplitude), α_k are the weighting coefficients to be determined and Φ_k is the multivariate polynomial basis. The latter is obtained by tensorization of monovariate polynomial basis given by the Askey scheme. A hyperbolic norm is adopted to select the PCE terms to keep in the expansion. The coefficients α_k are the solution of a least-square minimisation problem between N evaluations of the expensive model Y and its PCE approximation. For more details, the reader could refer to [7,10,11,12].

Kriging

The parametric part of each QoI can be approximated with a kriging surrogate model. In other words, a QoI α that depends on $\mathbf{x}$ can be approximated by [13]:

$$\alpha(\mathbf{x}) = \mathbf{g}(\mathbf{x})^T \boldsymbol{\beta} + Z(\mathbf{x})$$

where $\mathbf{g}$ is a set of regressive functions, often taken as polynomials of low order, $\boldsymbol{\beta}$ are the weighting coefficients and are solution of a least square problem, and Z is a zero-mean Gaussian process of variance σ^2, which covariance writes $E[Z(\mathbf{x}), Z(\mathbf{x}')] = \sigma^2 R(\boldsymbol{\theta}, \mathbf{x}, \mathbf{x}')$ with R the spatial correlation function of scaling parameter $\boldsymbol{\theta}$ and $\mathbf{x}$ and $\mathbf{x}'$ two points of the input space. To build the surrogate model, Q evaluations of the expensive model are necessary, i.e. Q inputs $\left(\mathbf{x}^{(j)}\right)$ and their evaluations $\left(\alpha^{(j)}\right) = \left(\alpha\left(\mathbf{x}^{(j)}\right)\right)$. For a detailed description of the Kriging and its practical implementation, the interested reader could refer to [7,10,13].

Kriging for a symmetrical problem

The possibility to improve the kriging process by taking into consideration the physical properties is discussed here. More specifically, the QoI considered here are symmetrical with respect to $k_v^{(b,2)} = k_h^{(b,2)}$. To consider this, three strategies are investigated in the following:

- A classic strategy: a classic kriging is constructed by choosing a regression function g and a correlation function, and no symmetric properties are considered.
- A half-design space restriction strategy: as the problem is symmetric, only points that satisfy $k_v^{(b,2)} \leq k_h^{(b,2)}$ are used for the kriging construction. For the prediction, half of the design space is directly reconstructed based on the symmetric property.
- A symmetrical regression strategy: the symmetric aspect of the problem introduced in the regression part directly. As an example, in dimension 2, if $\mathbf{g}$ is the second order polynomial regression function for a classical kriging, the symmetric regression function $\mathbf{g_s}$ would write:

$$\mathbf{g_s}(x_1, x_2) = \begin{cases} \beta_0 + \beta_1 x_1 + \beta_2 x_2 + \beta_3 x_1 x_2 + \beta_4 x_1^2 + \beta_5 x_2^2 & \text{if } x_1 \leq x_2 \\ \mathbf{g_s}(x_2, x_1) & \text{otherwise} \end{cases}$$

  with $x_1 = k_v^{(b,2)}$ and $x_2 = k_h^{(b,2)}$.

Hybrid formulation

The proposed hybrid surrogate model associates PCE and kriging, detailed in [7,10]. If Y denotes one QoI, i.e. $f^{(i)}$ or $a^{(i)}$, then it writes:

$$Y(\boldsymbol{\xi}, \mathbf{x}) = \sum_{k=0}^{P-1} a_k(\mathbf{x}) \Phi_k(\boldsymbol{\xi}) = \sum_{k=0}^{P-1} \left(\mathbf{g}^{(k)}(\mathbf{x})^T \boldsymbol{\beta}^{(k)} + Z^{(k)}(\mathbf{x})\right) \Phi_k(\boldsymbol{\xi})$$

Y is obtained by expanding it on a PCE, where PCE coefficients depend on the parametric vector $\mathbf{x}$. These coefficients are then approximated with a kriging surrogate model. Considering the training set, Q points $\left(\mathbf{x}^{(j)}\right)$ and N points $\left(\boldsymbol{\xi}^{(j)}\right)$ are generated. The final training set is obtained by tensorization of these two sets. For each point, the critical speeds and associated amplitudes are computed.

Exploitation of PCE coefficients

From the PCE expansion, one gets directly access to the mean and variance of the process, that depend directly on the vector **x** in this case. The interest of the current formulation is that the average and variance can be obtained on the full parametric space without additional MCS (as it would have been the case if a unique kriging surrogate model were built). It writes:

$$E[Y(\mathbf{x})] = a_0(\mathbf{x}) = \mathbf{g}^{(0)}(\mathbf{x})^T \boldsymbol{\beta}^{(0)} + Z^{(0)}(\mathbf{x})$$

$$\sigma^2_{Y(\mathbf{x})} = \sum_{k=1}^{P-1} a_k(\mathbf{x})^2 \left|\left|\Phi_k\right|\right|^2 = \sum_{k=0}^{P-1} \left(\mathbf{g}^{(k)}(\mathbf{x})^T \boldsymbol{\beta}^{(k)} + Z^{(k)}(\mathbf{x})\right)^2 \left|\left|\Phi_k\right|\right|^2$$

Similarly, the Sobol indices $S_i(\mathbf{x})$ are directly related to the PCE coefficients and are equal to [12]:

$$S_i(\mathbf{x}) = \frac{V_i(\mathbf{x})}{V\big(Y(\mathbf{x})\big)}$$

Where $V_i(\mathbf{x}) = \sum_{j \in v_i} \alpha_j(\mathbf{x})^2 \left|\left|\Phi_j\right|\right|^2$ with v_i the set of multivariate indices for which the only polynomials related to the variable i are present.

RESULTS

In this section, the results obtained are presented and commented. A first brief part is dedicated to the strategy adopted for the construction and validation of the hybrid surrogate models. Then, the three different kriging strategies are compared. Finally, a variance-based sensitivity analysis is performed.

Construction of the surrogate models

For the construction of the training set, the first input set related to the PCE is generated based on an LHS of N =250 points (250 values of $\boldsymbol{\xi}$). For the kriging, Q points are generated based on an LHS maximising a maximin criterion, and 4 different sizes are considered, namely $Q = [20, 40, 60, 80]$. The first 8 critical speeds and associated vibration amplitudes are computed for the $N \times Q$ configurations.

For 8 values of **x**, 500 reference points are got to validate the PCE parts. The PCE properties are tuned to ensure the minimum level of relative error over the 8×500 points.

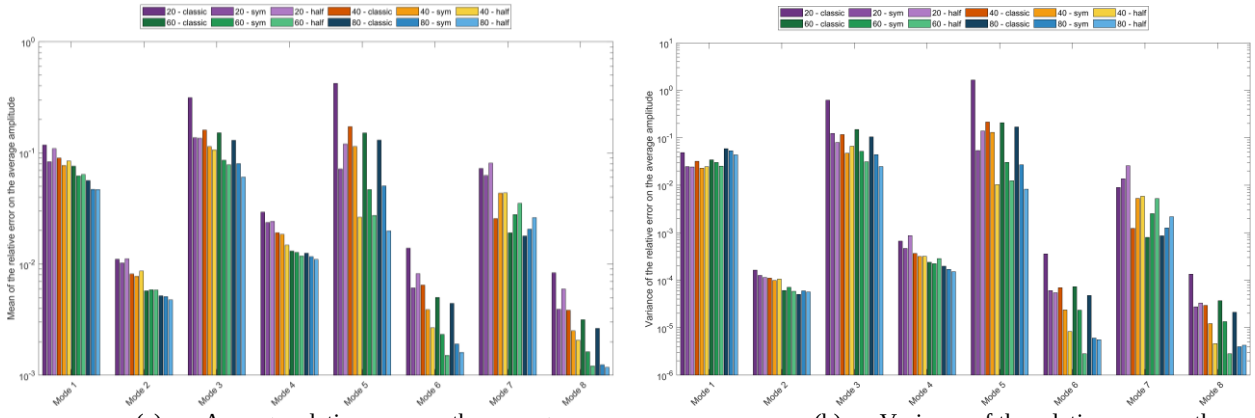

(a) - Average relative error on the average amplitude

(b) – Variance of the relative error on the average amplitude

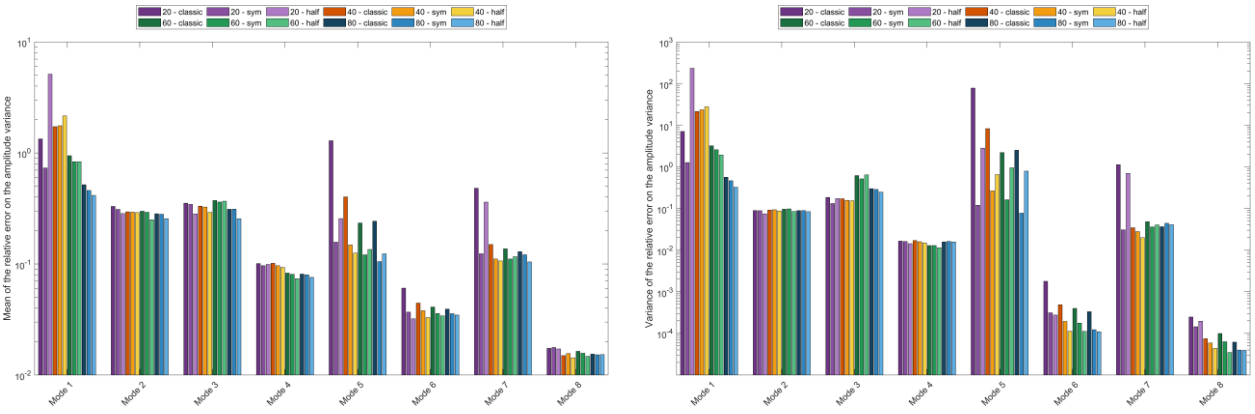

(c) – Average error on the amplitude variance

(d) – Variance of the relative error on the amplitude variance

Figure 3: Average (a) and variance (b) of the relative error on the mean vibration amplitudes and Average (c) and variance (d) of the relative error on the vibration amplitudes variance

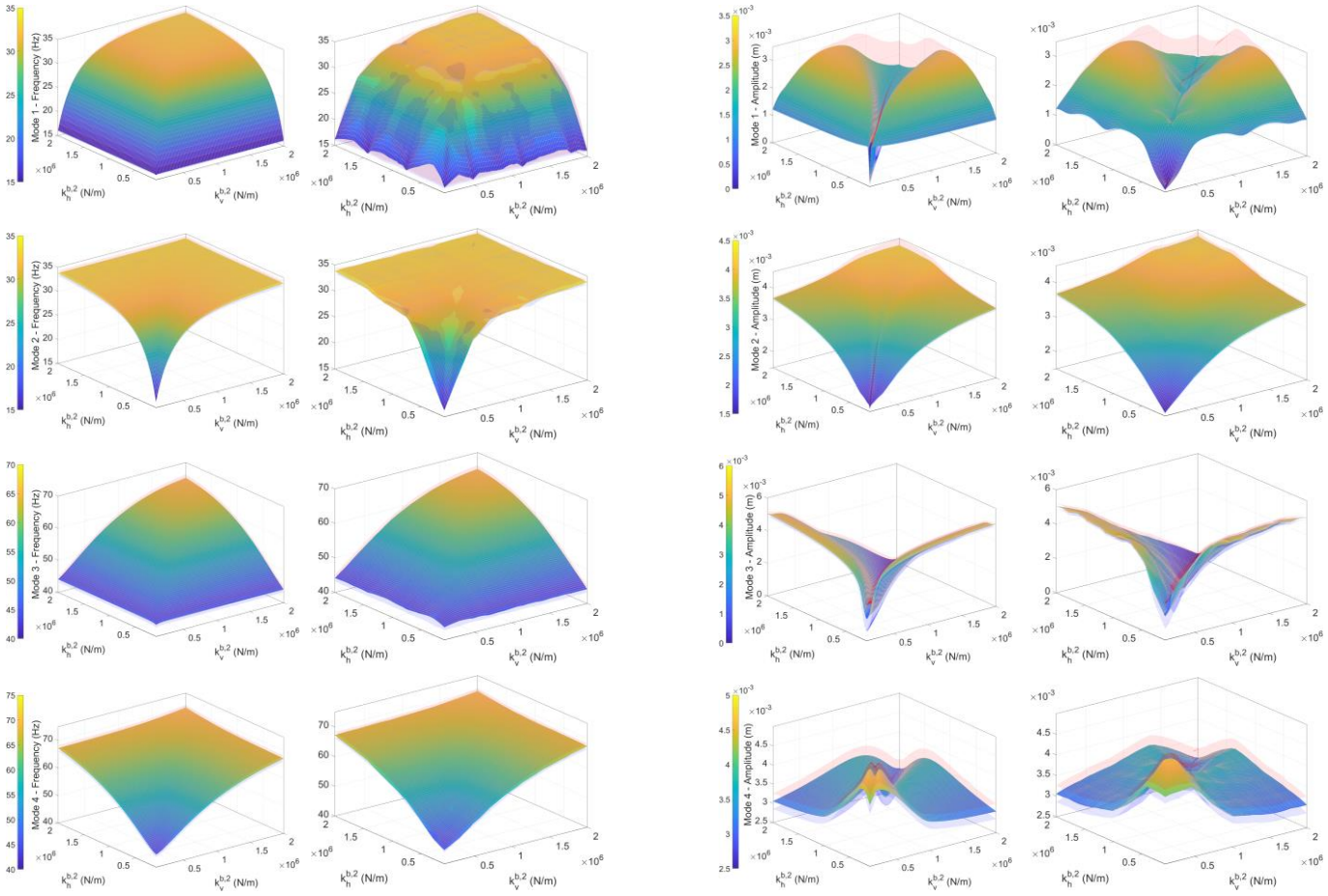

Figure 4: Evolution of the average and average ± standard deviation for the critical speeds (reference: first column, prediction: second column) and associated vibration amplitudes (reference: third column, prediction: fourth column)

The second step consists in the construction of the kriging surrogate models for each PCE coefficient. To validate this part, the average and variance of the 8 critical speeds $f^{(i)}$ and associated vibration amplitudes $a^{(i)}$ are computed over a grid of 100×100, and kriging prediction are compared to these reference values. The comparison of the kriging strategies is presented in the following.

Comparison of the kriging strategies

The error on the average and variance of the critical speeds and associated vibration amplitudes over the 100×100 grid is computed. This error is defined as:

$$Error(\mathbf{x}) = \frac{r_p(\mathbf{x}) - r_{ref}(\mathbf{x})}{|r_{ref}(\mathbf{x})|}$$

With r_p the prediction of the average (variance resp.) and r_{ref} the reference of the average (variance resp.) of the considered QoI. It is computed for the 8 critical speeds $f^{(i)}$ and the associated vibration amplitudes $a^{(i)}$ and for the different cases (4 DoE sizes and 3 kriging strategies). Means and variances of this error over the 100×100 grid are computed. They are displayed for the vibration amplitudes in Figure 3. Results are similar for the critical speeds but are not given here for the sake of concision.

The following conclusions can be drawn:

- Errors vary a lot from one mode to another, and they tend to be lower for forward modes (even number) than for backward modes (odd number). This is explained by the fact that amplitudes for the backward modes are almost zero for equal stiffness $k_v^{(b,2)} = k_h^{(b,2)}$, which tends to increase the relative error.
- When the DoE size increases, the errors decrease on average and variance. The convergence is more or less quick depending on the mode.
- Globally, the classic kriging strategy is the worst strategy, and the half-design strategy performs better than the others and gives error level that can be several order of magnitude bellow. It is particularly clear on the average amplitudes for higher modes. Or, for example, for the 20 points case, the symmetric strategy performs better than the others and it gives better results than the classic strategy with 80 points. This demonstrates the drastic numerical cost reduction such strategy can bring.

When looking at the difference in prediction between the different strategies, it appears that the main differences between the different strategies are around the line $k_v^{(b,2)} = k_h^{(b,2)}$. The classic kriging strategy is in fact unable to catch the sharp evolutions of the amplitudes around this axis, especially for backward modes where amplitudes almost jump to 0 around this line. On the other hand, the two other strategies were able to capture this sharp evolution due to their construction (symmetry imposed either in the regression or in the restriction of the DoE).

As a conclusion, the three strategies perform well globally. However, the half-design and symmetric regression strategies perform a better and should be used compared to the classic kriging strategy. Moreover, the half-design strategy required twice less training points and so should be chosen preferably as it represents the best compromise between accuracy and numerical cost. These results demonstrate that adding information about the problem properties in the kriging construction or in the DoE construction improves substantially the kriging efficiency and reduces drastically the size of the required training set.

Finally, the results obtained for prediction the vibration amplitudes and critical speeds are given in Figure 4. Only the first four modes are given for the sake of concision. The coloured surface corresponds to the average value of the QoI and red and blue surfaces correspond to the average $\pm$ the standard deviation. Results are given with the half-design space strategy with a training set of 30 points for the kriging. One could clearly see here the good agreement between the predictions and the reference case, which illustrates the efficiency of the hybrid meta-model to surrogate the behaviour of the full rotor.

Variance-based sensitivity analysis based on Sobol indices

A sensitivity analysis is now conducted on the rotor to get insights in the influence played by the different random parameters on the rotor dynamics. The Sobol indices can be deducted directly from the PCE coefficients without any additional cost, which makes this type of analysis very interesting in complement of PCE. As a reminder, Sobol indices are indicator that makes possible to state on the influence of an input variable on the output variance. If the Sobol index associated to one variable is close to 1, then this parameter has no influence on the output variance. On the contrary, if the Sobol index, then this parameter is highly influential. First order Sobol indices are given for the first four modes in Figure 5, for the critical speeds and associated vibration amplitudes.

At a first glance, one could clearly see that the Sobol indices strongly depend on the considered mode. Indeed, one could see that the thickness of the first disc e_1 has a strong influence on the vibration amplitudes associated to the mode 4, whereas it has a low influence on the vibration amplitudes of mode 1. They are also different for the critical speeds and the vibration amplitudes. Indeed, for example, the thickness of the first disc e_1 has a strong influence on the critical speeds of mode 1 (equal to 0.5 over almost the whole domain) whereas it has a limited effect on the vibration amplitude (almost 0 over the whole domain). Then, the Sobol indices also strongly depend on the value of the stiffness $k_v^{(b,2)}$ and $k_h^{(b,2)}$: see for example $S_{k_h^{(b,1)}}$ for the vibration amplitude where it has large values for $k_v^{(b,2)} = k_h^{(b,2)}$ and low values otherwise.

More precisely, the following conclusions can be drawn for each mode:

- Mode 1: for low stiffness values, thicknesses of the discs 3 and 4 have a large influence on the critical speed. For higher values, the Young modulus and the thickness of the first disc have the higher influence. Considering the vibration amplitudes, far from $k_v^{(b,2)} = k_h^{(b,2)}$, the thickness of discs 3 and 4 have the largest contributions. Otherwise, the two stiffness $k_v^{(b,1)}$ and $k_h^{(b,1)}$ are the most influential parameters.
- Mode 2: the parameters that drive the critical speeds are the Young modulus, the thickness of the first disc and the stiffness $k_h^{(b,1)}$. The parameters that drive the vibration amplitudes are the thickness of the disc 3 when far from $k_v^{(b,2)} = k_h^{(b,2)}$, and are the thickness of the first disc, the stiffness $k_h^{(b,1)}$ and the stiffness $k_v^{(b,1)}$ otherwise.
- Mode 3: The critical speed is mostly driven by the thickness of the first disc. The vibration amplitudes are driven by the two stiffnesses when $k_v^{(b,2)} = k_h^{(b,2)}$ and by the thickness of the first disc otherwise.
- Mode 4: the thickness of the first disc drives mostly the critical speed as well as the vibration amplitudes.

More generally, the influence of a disc thickness on a mode depends strongly on its location. If the former is located on a node (anti-node, resp.) of the mode, then it will have a low (high, resp.) influence on the critical speeds. Considering the vibration amplitudes, if $k_v^{(b,2)} = k_v^{(b,2)}$, then stiffness $k_v^{(b,1)}$ and $k_h^{(b,1)}$ drive the symmetrical property of the rotor and so if they are different then the rotor becomes asymmetric and have large experience important vibrations.

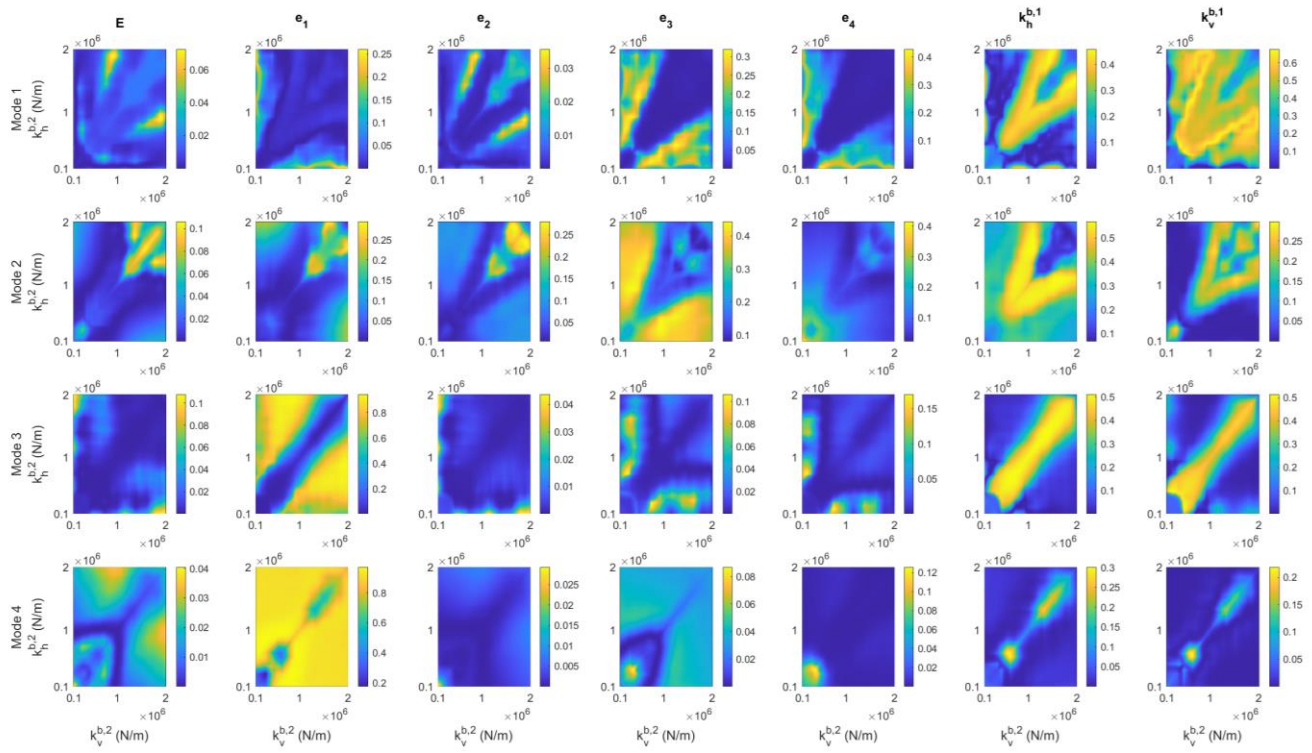

(a)

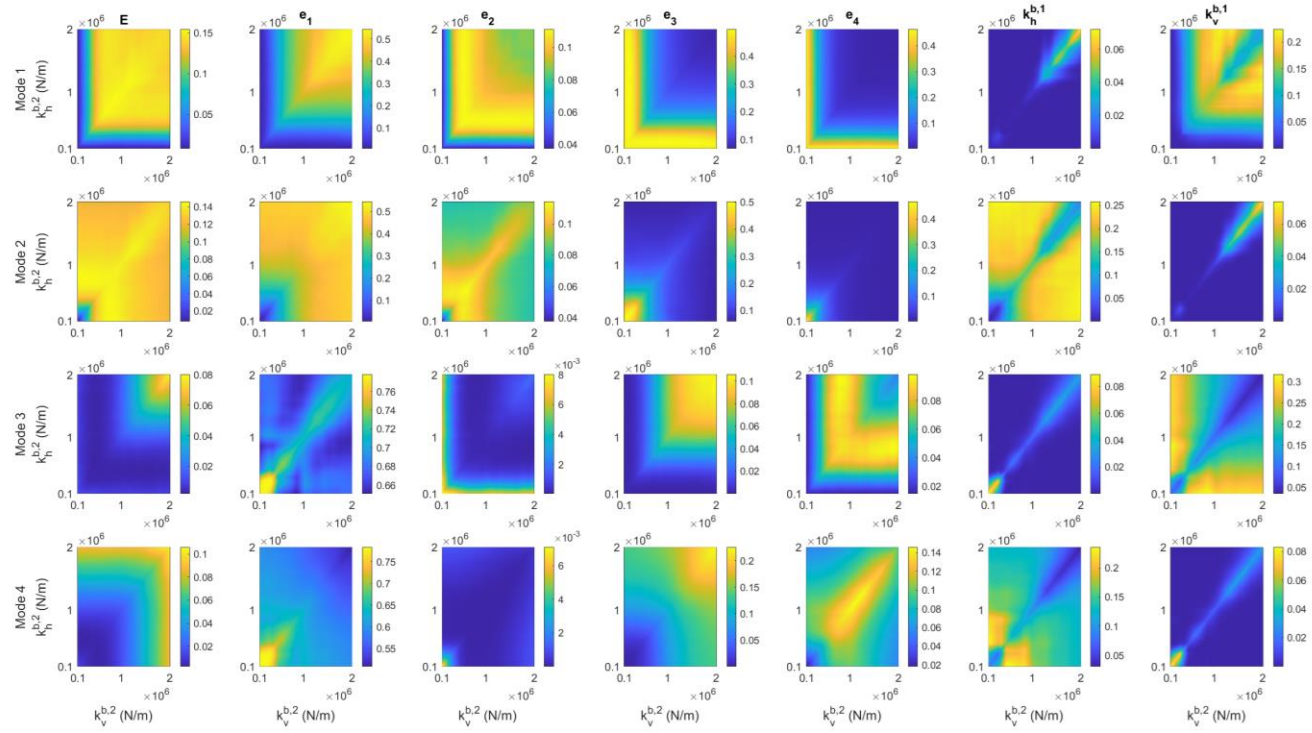

(b)

Figure 5: First order Sobol indices for the vibration amplitudes (a) and critical speeds (b)

CONCLUSION

In the present work, a hybrid surrogate model has been used to predict accurately and efficiently the critical speeds and associated vibration amplitudes of the forward and backward modes of a rotor. The potential of such approach to deal with large models with numerous uncertainties is demonstrated.

Random parameters are modelled through a PCE and parametric parameters with kriging. The combination of the two methods makes possible to consider a high number of uncertainties that can be of different natures. Moreover, as the PCE coefficients are directly predicted with kriging, stochastic properties, as mean and variance, and Sobol indices

can directly be estimated without additional costly MCS. This makes the method very efficient to identify the impact of the parametric variables on the stochastic response of the rotor. In a context of design, this approach is very promising. Finally, Sobol indices are used to perform a sensitivity analysis and insights in the rotor dynamics and the influence of the different parameters is assessed.

Three kriging strategies have been compared and it is shown that introducing known properties about symmetry in the kriging construction improves its efficiency, both in terms of accuracy and convergence speed. It demonstrates the relevance of introducing the expertise that engineers and researchers have gain so far directly in the surrogate model construction, and of developing grey-box models for structural dynamics.

REFERENCES

[1] Sarrouy, E., Dessombz, O., & Sinou, J. J. (2012). Stochastic analysis of the eigenvalue problem for mechanical systems using polynomial chaos expansion—application to a finite element rotor. *Journal of vibration and acoustics*, *134*(5).

[2] Didier, J., Faverjon, B., & Sinou, J. J. (2012). Analysing the dynamic response of a rotor system under uncertain parameters by polynomial chaos expansion. *Journal of Vibration and Control*, *18*(5), 712-732.

[3] Garoli, G. Y., & de Castro, H. F. (2020). Generalized polynomial chaos expansion applied to uncertainties quantification in rotating machinery fault analysis. *Journal of the Brazilian Society of Mechanical Sciences and Engineering*, *42*(11), 1-15.

[4] Wang, D., Hua, C., Dong, D., He, B., & Lu, Z. (2018). Crack parameters identification based on a kriging surrogate model for operating rotors. *Shock and Vibration*, *2018*.

[5] Sinou, J. J., Nechak, L., & Besset, S. (2018). Kriging metamodeling in rotordynamics: Application for predicting critical speeds and vibrations of a flexible rotor. *Complexity*, *2018*.

[6] Silva Barbosa, J., Campanine Sicchieri, L., Dourado, A. D. P., Cavalini Jr, A. A., & Steffen Jr, V. (2021). Kriging Approach Dedicated to Represent Hydrodynamic Bearings. *Journal of Engineering for Gas Turbines and Power*, *143*(6), 061016.

[7] Denimal, E., Nechak, L., Sinou, J. J., & Nacivet, S. (2018). A novel hybrid surrogate model and its application on a mechanical system subjected to friction-induced vibration. *Journal of Sound and Vibration*, *434*, 456-474.

[8] Denimal, E., Sinou, J. J., & Nacivet, S. (2021). Prediction of Squeal Instabilities of a Finite Element Model Automotive Brake With Uncertain Structural and Environmental Parameters With a Hybrid Surrogate Model. *Journal of Vibration and Acoustics*, *144*(2), 021006.

[9] Friswell, M. I., Penny, J. E., Garvey, S. D., & Lees, A. W. (2010). *Dynamics of rotating machines*. Cambridge university press.

[10] Denimal, E., & Sinou, J. J. (2021). Advanced kriging-based surrogate modelling and sensitivity analysis for rotordynamics with uncertainties. *European Journal of Mechanics-A/Solids*, 104331.

[11] Xiu, D., & Karniadakis, G. E. (2002). The Wiener--Askey polynomial chaos for stochastic differential equations. *SIAM journal on scientific computing*, *24*(2), 619-644.

[12] Sudret, B. (2008). Global sensitivity analysis using polynomial chaos expansions. *Reliability engineering & system safety*, *93*(7), 964-979.

[13] Lophaven, S. N., Nielsen, H. B., & Søndergaard, J. (2002). *DACE: a Matlab kriging toolbox* (Vol. 2). IMM, Informatics and Mathematical Modelling, The Technical University of Denmark.

Acknowledgement

E. Denimal acknowledges the financial support of Rennes Metropole. J-J. Sinou acknowledges the support of the Institut Universitaire de France.